Cytotechnology (2005) 48:1–13
DOI 10.1007/s10616-005-1920-6

Analysis of methylglyoxal metabolism in CHO cells grown in culture

Sarocha Kingkeohoi and Frank W.R. Chaplen*
*Department of Biological and Ecological Engineering, Oregon State University, 116 Gilmore Hall, Corvallis, OR 97331-3906, USA; *Author for correspondence (e-mail: chaplenf@engr.orst.edu; phone: +1-541-737-1015; fax: +1-541-737-2082)*

Received 15 September 2004; accepted in revised form 29 July 2005

Key words: CHO cell, Inhibitor, Metabolism, Metabolite, Methylglyoxal

Abstract

Recent evidence suggests that several unknown or ill-characterized factors strongly influence cell growth and function in culture. Isolating these factors is necessary in order to maximize culture productivities. Methylglyoxal (MG), a potent protein and nucleic acid modifying agent, has been identified as a player in the signaling pathways associated with cell death and is known to be detrimental to cultured cells. This compound is produced in all mammalian systems by spontaneous phosphate elimination from glycolytic pathway intermediates. A kinetic model that qualitatively describes the cellular distribution of protein-associated MG in the absence of enzymatic adduct formation predicted far lower levels of reversibly bound MG than measured in cultured CHO cells. This suggests that the targeted modification of proteins through enzymatically mediated mechanisms is a significant sink for cellular methylglyoxal. The model was validated with measurements of carbon flux through the glyoxalase pathway to D-lactic acid, a unique end product of MG metabolism in mammalian systems. Fluxes to D-lactic acid of up to 16.8 mmol ml-packed cells^{-1} day^{-1} were measured with CHO cells grown in batch culture or 100-fold more than found in normal tissues.

Introduction

The ability of cultured mammalian cells to produce high titers of consistent product is influenced by many known chemical factors in the bioreactor, including media composition, nutrient concentrations, and autologously made inhibitors of cell growth and function. Major examples of the latter are the toxic by-products ammonium ion and lactate, still believed to be the principal inhibitors produced by animal cell cultures (Miller and Blanch 1991; Anderson and Goochee 1995). It is also evident that other unknown or ill-characterized factors that strongly affect cell growth and function exist, especially in high-intensity perfusion and fed-batch cultures (Bibila and Robinson 1995).

Methylglyoxal (MG) is a potent protein and nucleic acid modifying agent found in all mammalian systems as a consequence of energy metabolism. MG is produced through spontaneous phosphate elimination from glycolytic pathway intermediates. MG levels also respond to signaling events associated with cell death (Van Herreweghe et al. 2002), indicating that anabolic activities for MG production may be present in mammalian systems as they are in bacteria, although that is yet to be demonstrated. The principal catabolic activity for MG is the glyoxalase pathway, which consists of glyoxalase I (GLO1;

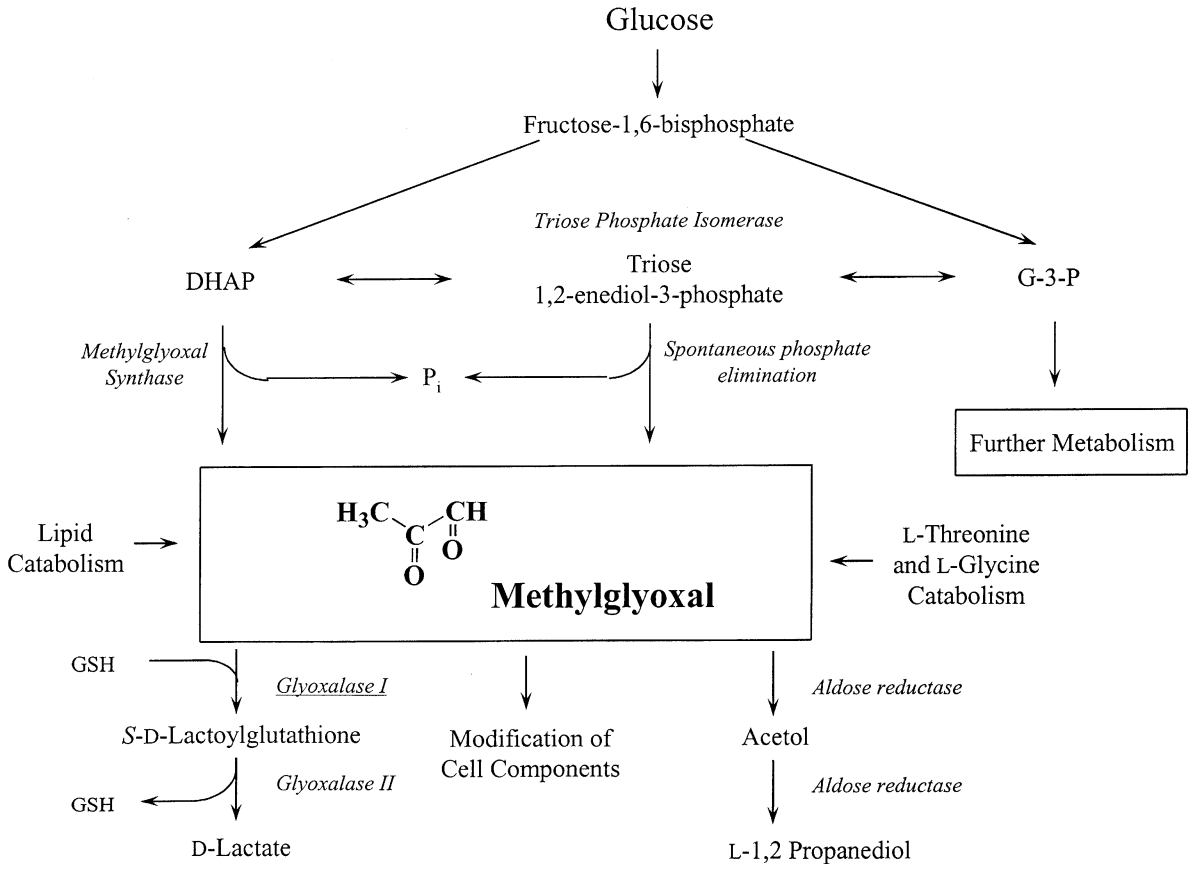

Figure 1. Methylglyoxal metabolism in mammalian systems. DHAP, dihydroxyacetone phosphate; G-3-P, glyceraldehyde-3-phosphate. Aldose reductase route for MG catabolism is not shown. See Chaplen et al. (1998) for a full review of MG and MG metabolism in animal cell culture.

Figure 1) and glyoxalase II (GLO2); reduced glutathione (GSH) is a required co-enzyme for this pathway. Aldose reductases are secondary catabolic activities that become important as cellular GSH is depleted, such as under conditions of oxidative stress (Vander Jagt et al. 2001). MG-mediated cell death is tightly coupled to interactions between energy metabolism, free MG levels, reactive oxygen species (ROS), and the phosphorylation status of GLO1 (Van Herreweghe et al. 2002). Multiple cell death pathways involving MG as a signal element appear to exist. Increased endogenous MG directly initiates cell death signaling cascades in some instances, whilst in others it occurs as a consequence of cell death activation. Specific pathway activation is cell-line dependent and results in either necrosis- or apoptosis-like end states (Du et al. 2000; Sakamoto et al. 2000; Godbout et al. 2001; Vander Jagt et al. 2001).

Recent evidence suggests that MG is a signal molecule involved in the processes regulating apoptosis or programmed cell death (PCD). Earlier studies demonstrate that relatively small increases in the level of endogenously produced MG decrease cell viability in Chinese hamster ovary (CHO) cells (Chaplen et al. 1996a) under growth conditions found in industrial cell culture. Here we develop a kinetic model that qualitatively describes the cellular distribution of protein-associated MG in the absence of enzymatic adduct formation. Measurements of carbon flux through the glyoxalase pathway to D-lactic acid, a unique end product of MG metabolism in mammalian systems were used to validate the model, which predicted far lower levels of reversibly bound MG than measured in cultured

CHO cells. This suggests that the targeted modification of proteins by phosphorylated GLO1 or other as yet unidentified enzymatically mediated mechanisms is a significant sink for cellular MG. The model also supports observations that CHO cells have higher levels of MG than normal tissues further adding to the possible significance of MG to industrial cell cultures.

Materials and methods

Chemicals and solutions

All chemicals were of reagent grade. D-Lactate dehydrogenase (*Staphylococcus epidermis*), nicotinamide adenine dinucletotide (NAD^+), diethylenetriaminepentaacetic acid (DETAPAC), glycine, and D-lactate (lithium salts) were purchased from Sigma – Aldrich Co.Ltd. 5-Methylquinoxaline (5-MQ), *o*-phenylenediamine (*o*-PD) were made as previously described (Chaplen et al. 1996b).

Cell culture

Chinese hamster ovary cells expressing recombinant tissue plasminogen activator (ATCC CRL 9606) were grown in Dulbecco's Modified Eagle Medium or D-MEM high glucose (GIBCO/BRL/Life Technologies) as described elsewhere (Chaplen et al. 1996b). Cell counts and cell volumes were determined as described elsewhere (Chaplen et al. 1996b).

Methylglyoxal assay

Free MG was assayed in the medium and cells as described elsewhere (Chaplen et al. 1996b).

D-Lactate assay

The D-lactate assay used was a modification of the D-lactate assay used for human blood samples (McLellan et al. 1992) and L-lactate Sigma diagnostic procedure No.826-UV (Sigma-Aldrich Co.). A 3 mg/ml stock solution of D-lactate was prepared. Hydrazine sulfate (26 mg/ml)/glycine (0.6 M) buffer was prepared and the pH adjusted to 9.2 by 5 M KOH. D-Lactate dehydrogenase solution was prepared at a concentration of 1000 U/ml just prior to use. DETPAC stock solution was made at 0.4 mg/ml in distilled water. The final assay mixture was 6 ml of 5 mg/ml NAD^+ in glycine–hydrazine buffer, 0.7 ml distilled water and 0.3 ml of D-lactate dehydrogenase. A 1:1 ratio of sample media and 8% (w/v) perchloric acid was mixed, incubated on ice for 10 min, and centrifuged at $4000 \times g$ discarding any precipitate. The final assay volume was 3 ml (2.88 ml assay mixture, 20 μl DETPAC and 100 μl sample). This was incubated in a 37 °C water bath for 30 min. Fluorescence was measured at 450 nm under excitation at 350 nm in a Perkin-Elmer MPF 2A Fluorescence Spectrophotometer.

D-Lactate flux assay

CHO cells were seeded at 2×10^6 cells per T-150 tissue culture flask in 30 ml of D-MEM high glucose. Three flasks were sacrificed at each time point (0, 4, 20, 30, 45, 65, 75, 90 h). D-Lactate concentrations were determined as described above. The packed cell volume in each T-flask was determined as described above and used to normalize the D-lactate concentrations. D-Lactate flux was calculated as (Value at time point − Value at previous time point)/(Time elapsed between samples).

Rate constants for methylglyoxal degradation

MG (45 mM) was incubated in 50 mM potassium phosphate buffer, pH 7.4, for 24 h at 37 °C. Free MG in solution was measured at various times by derivatizing with *o*-PD followed by HPLC analysis (Chaplen et al. 1998). The first- and second-order rate constants for disappearance of MG were determined by parameter estimation.

Data analysis and kinetic modeling

Parameter estimation for determining the rate constants of MG degradation in phosphate buffer and the derivatization of MG by *o*-PD was done using an equation solver (Microsoft Excel, Microsoft Corp., Redmond, WA). Mathematical modeling of interactions between MG and the

various amino acids was done using the numerical integration functions of the same program.

Model theory and development

Model 1: *Methylglyoxal interactions with proteins in vitro*

Interactions between MG and proteins were modeled because proteins are a major modification target for MG *in vivo*. The model was validated using experimental data originally obtained from a reaction system consisting of 100 μM MG and 1 mM bovine serum albumin (BSA) at physiological pH (7.0) and temperature (37 °C) as reported in Lo et al. (1994). The principal modification targets in proteins are arginine, lysine or cysteine residues. The amounts of arginine, lysine and cysteine present in 1 mM BSA are 2300 μM, 6100 μM and 100 μM, respectively. These numbers were derived from the amino acid sequence of BSA (Jocelyn 1977), and by assuming an average molecular weight for BSA of 70 kDa, and for amino acid residues of 121 Da.

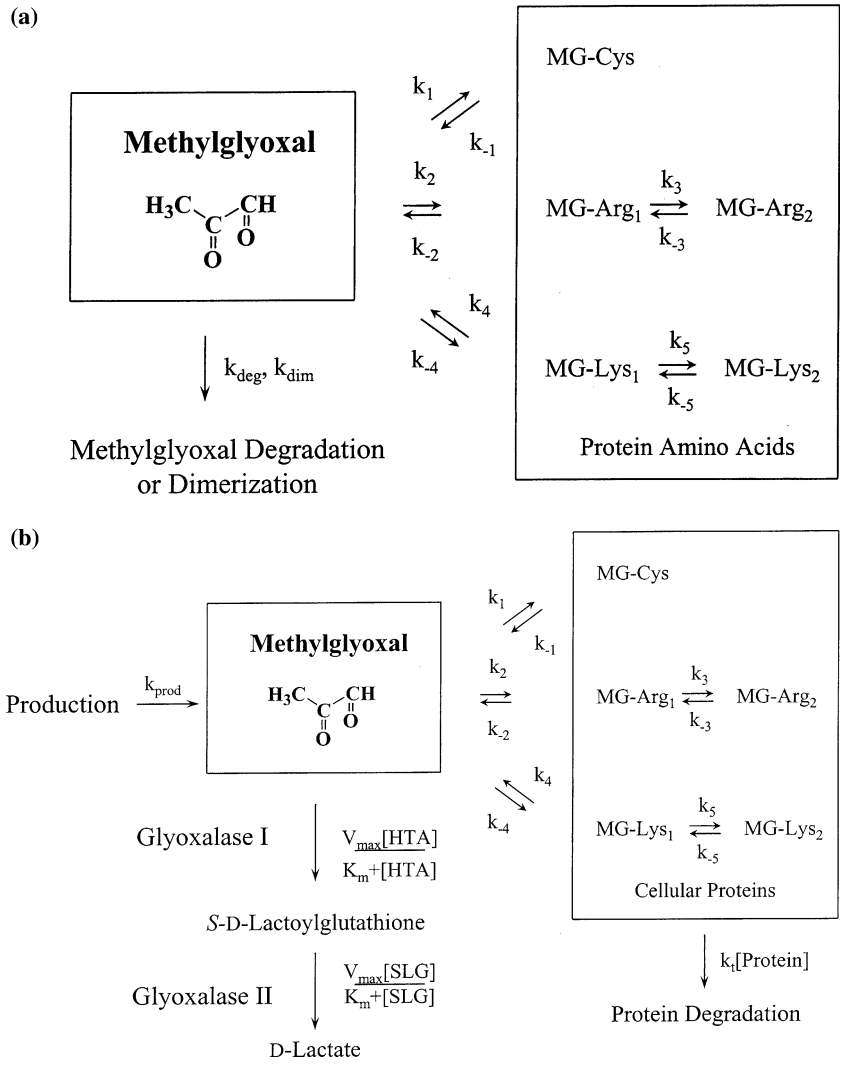

Figure 2. Model schematics. (a) Model #1: MG interactions with proteins *in vitro*. (b) Model #2: MG interactions with proteins *in vivo*.

The rate constants used in the model were those of the reaction of MG with the *N*α-acetylamino acid forms of each amino acid, data also taken from Lo et al. (1994). Figure 2a shows a model schematic. The rate constants for cysteine are $k_1 = 1.4\times10^{1}$ M^{-1} s^{-1} and $k_{-1} = 7.5\times10^{-3}$ s^{-1}; the rate constants for arginine are $k_2 = 8.5\times10^{-3}$ M^{-1} s^{-1}, $k_{-2} = 4.4\times10^{-6}$ s^{-1}, $k_3 = 6.7\times10^{-4}$ s^{-1} and $k_{-3} = 1.9\times10^{-4}$ s^{-1}; and the rate constants for lysine are $k_4 = 6.8\times10^{-3}$ M^{-1} s^{-1} and $k_{-4} = 5.0\times10^{-4}$ s^{-1}, $k_5 = 1.9\times10^{-2}$ M^{-1} s^{-1} and $k_{-5} = 2.0\times10^{-3}$ s^{-1}. The rate constants for cysteine were determined based on the concentration of the non-hydrated form of MG. The forward rate constant for the cysteine reaction (k_1) originally reported in Lo et al. (1994) was modified by assuming that the non-hydrated form of MG represents ca. 1.9% of the total free MG concentration at equilibrium. The rate constants for arginine and lysine were determined based on the total free MG concentration. The degradation and dimerization of free MG that occurs under the conditions of the reported study must also be accounted for to provide good agreement with the *in vitro* data. The kinetics of MG degradation was determined as described above. MG degradation was modeled as combined first order (degradation) and second order (dimerization) reactions. The rate constant for degradation was $k_{deg} = 3.0\times10^{-6}$ s^{-1}; the rate constant for dimerization was $k_{dim} = 4.9\times10^{-4}$ M^{-1} s^{-1}. Equations (1)–(9) show the model in differential equation form. C_1 is the hemithioacetal formed between *N*α-acetylcysteine and MG; A_1 is *N*α-acetylarginine-MG glycosylamine; A_2 is 4,5-dihydroxy-5-methylimidazolidine; L_1 is *N* α-acetyllysinemethylglyoxal glycosylamine; L_2 is bis(*N*α-acetyllysine)methylglyoxal glycosylamine.

$$\frac{d[MG]}{dt} = -k_1[C][MG] + k_{-1}[C_1] - k_2[A] \times [MG] + k_{-2}[A_1] - k_4[L][MG] + k_{-4}[L_1] - k_6[MG] - k_7[MG] \times [MG] \quad (1)$$

$$\frac{d[C]}{dt} = -k_1[C][MG] + k_{-1}[C_1] \quad (2)$$

$$\frac{d[A]}{dt} = -k_2[A][MG] + k_{-2}[A_1] \quad (3)$$

$$\frac{d[L]}{dt} = -k_4[L][MG] + k_{-4}[L_1] \quad (4)$$

$$\frac{d[C_1]}{dt} = k_1[C][MG] - k_{-1}[C_1] \quad (5)$$

$$\frac{d[A_1]}{dt} = k_2[A][MG] - k_{-2}[A_1] - k_3[A_1] + k_{-3}[A_2] \quad (6)$$

$$\frac{d[L_1]}{dt} = k_4[L][MG] - k_{-4}[L_1] - k_5[L_1][L] + k_{-5}[L_2] \quad (7)$$

$$\frac{d[A_2]}{dt} = k_3[A_1] - k_{-3}[A_2] \quad (8)$$

$$\frac{d[L_2]}{dt} = k_5[L_1][L] - k_{-5}[L_2] \quad (9)$$

An understanding of the tertiary structure of BSA in solution was also important for maximizing agreement between the model and the available data. BSA in solution is conformationally dynamic (Jocelyn 1977), which would effectively expose most residues to MG modification. Therefore, all arginine and lysine residues were treated as being available for reaction with MG. Most cysteine residues in BSA are in the cystine form as they are involved in disulfide bond formation. The number reported for free cysteine residues is generally one (Jocelyn 1997). Model predications for reversibly bound MG were the sum of cysteine and the initial modification steps for arginine and lysine. Secondary reactions at arginine and lysine residues are effectively irreversible based on the available rate constant data and described secondary structures (Bourajjaj et al. 2003).

Model 2: *Methylglyoxal interactions with proteins in vivo*

The model described in the previous section was extended to consider interactions between intracellular proteins and MG. The total concentrations of arginine, lysine and cysteine present in the cell were assumed 70.5 μmol ml-packed-cell^{-1}, 105 μmol ml-packed-cell^{-1} and 39.74 μmol ml-packed-cell^{-1}, respectively. The concentration of each amino acid was determined from the overall amino acid composition of proteins in animal cells (Xie and Wang 1994). To determine the cysteine residue concentration, the ratio of cysteine to cystine residues (11.5:1) was taken to be the average of the reported ratios for 85 enzymes and other proteins (Jocelyn 1977). The protein concentration in animal cells is approximately 180 g/l (Alberts et al. 1994) and this was used, along with an average amino acid molecular weight of 121 Da, to determine the overall amino acid concentrations. The degradation of MG present in the Model 1 was neglected since this term is negligible at the low free MG concentrations present in the cell.

Three additional terms were added to Model 1 to account for MG metabolism. Figure 2b shows terms for MG production, MG catabolism by the glyoxalase pathway and MG-modified protein degradation or turnover. MG production was treated as a simple zero order term. MG catabolism by the glyoxalase pathway was assumed to follow Michaelis–Menten kinetics. $V_{\max}$ for glyoxalase I was estimated based on measured activities from cultured CHO cells (310 μmol-product/(min mg-total-protein); Chaplen et al. 1996a), K_{m} was the average of several reported K_{m} for mammalian systems (200 μM; Thornalley 1990). The true substrate for glyoxalase I is the hemithioacetal formed between MG and reduced glutathione. K_{eq} for hemithioacetal formation has been measured as 333 M^{-1} (Vander Jagt et al. 1972). Reduced glutathione was assumed present at the same level as for red blood cells (2 μmol ml-packed-cell^{-1}; Thornalley 1990). $V_{\max}$ for glyoxalase II was estimated based on the measured activities for CHO cells (30 μmol-substrate consumed/(min mg-total-protein); this study), K_{m} was the average of several reported K_{m} for mammalian systems (230 μM; Thornalley 1990). Finally, protein degradation or turnover rate was assumed first order in protein concentration, with the turnover rate constant, k_t. The model in differential equation form consisted of Equations (10)–(20). MGA in Equation (10) is the MG produced through MG anabolism; HTA is the hemithioacetal substrate of glyoxalase I. SLG in equations (11 and 12) is the product of the glyoxalase I reaction (S-D-lactoylglutathione) and DL in equation (12) is the product of the glyoxalase II reaction (D-lactate).

$$\frac{d[\mathrm{MG}]}{dt} = \mathrm{MGA} - \frac{V_{\max\ \mathrm{GLO1}}[\mathrm{HTA}]}{K_{mGLO1} + [\mathrm{HTA}]} - k_1[\mathrm{C}][\mathrm{MG}] + k_{-1}[\mathrm{C_1}] - k_2[\mathrm{A}] \times [\mathrm{MG}] + k_{-2}[\mathrm{A_1}] - k_4[\mathrm{L}][\mathrm{MG}] + k_{-4}[\mathrm{L_1}] \quad (10)$$

$$\frac{d[\mathrm{SLG}]}{dt} = \frac{V_{\max\ \mathrm{GLO1}}[\mathrm{HTA}]}{K_{mGLO1} + [\mathrm{HTA}]} - \frac{V_{\max\ \mathrm{GLO2}}[\mathrm{SLG}]}{K_{mGLO2} + [\mathrm{SLG}]} \quad (11)$$

$$\frac{d[\mathrm{DL}]}{dt} = \frac{V_{\max\ \mathrm{GLO2}}[\mathrm{SLG}]}{K_{mGLO2} + [\mathrm{SLG}]} \quad (12)$$

$$\frac{d[\mathrm{C}]}{dt} = -k_1[\mathrm{C}][\mathrm{MG}] + k_{-1}[\mathrm{C_1}] \quad (13)$$

$$\frac{d[\mathrm{A}]}{dt} = -k_2[\mathrm{A}][\mathrm{MG}] + k_{-2}[\mathrm{A_1}] \quad (14)$$

$$\frac{d[\mathrm{L}]}{dt} = -k_4[\mathrm{L}][\mathrm{MG}] + k_{-4}[\mathrm{L_1}] \quad (15)$$

$$\frac{d[\mathrm{C_1}]}{dt} = k_1[\mathrm{C}][\mathrm{MG}] + k_{-1}[\mathrm{C_1}] - k_t[\mathrm{C_1}] \quad (16)$$

$$\frac{d[\mathrm{A_1}]}{dt} = k_2[\mathrm{A}][\mathrm{MG}] - k_{-2}[\mathrm{A_1}] - k_3[\mathrm{A_1}] + k_{-3}[\mathrm{A_2}] - k_t[\mathrm{A_1}] \quad (17)$$

$$\frac{d[L_1]}{dt} = k_4[L][MG] - k_{-4}[L_1] - k_5[L_1][L] + k_{-5}[L_2] - k_t[L_1] \quad (18)$$

$$\frac{d[A_2]}{dt} = k_3[A_1] - k_{-3}[A_2] - k_t[A_2] \quad (19)$$

$$\frac{d[L_2]}{dt} = k_5[L_1][L] - k_{-5}[L_2] - k_t[L_2] \quad (20)$$

Results

Modeling MG interactions with proteins in vitro

MG, a biogenic dicarbonyl that has been directly linked to adducts or advanced glycation end-product (AGE) formation in human tissues (Westwood et al. 1994; Ahmed et al. 1997; Uchida et al. 1997; Shinohara et al. 1998) and has recently been identified (along with glyoxalase I) as a key regulator of necrotic cell death in fibrosarcoma L929 cells (Van Herreweghe et al. 2002). This compound at the cellular level exists as a complex and heterogeneous mixture of free and bound forms. Proteins are a major target of MG and are modified in a series of reversible (bound MG considered to be in dynamic equilibrium with free MG at cellular time-scales) and irreversible reactions at cysteine, arginine and lysine residues. Hemithioacetal formation at cysteine residues is reversible (Lo et al. 1994), although recent evidence suggests that irreversible cysteine-derived adducts form under physiological conditions and are enzymatically mediated (Van Herreweghe et al. 2002). Arginine and lysine modification results in AGE formation via Schiff's base and Amadori rearrangement product intermediates and is believed to be an important signal for senescent protein degradation (Westwood and Thornalley 1996). The initial reaction steps are reversible and involve non-enzymatic Schiff's base formation between the aldehyde or ketone moiety of MG and protein amine groups (Shamsi et al. 1998), followed by a rearrangement to more stable,

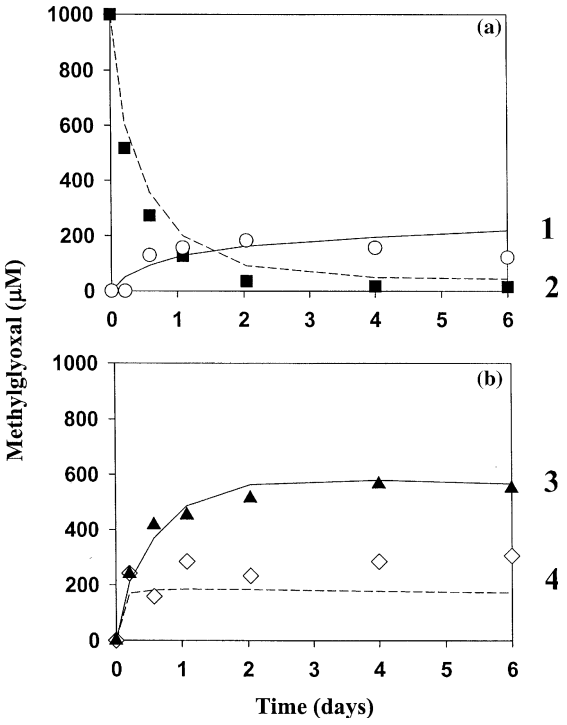

Figure 3. Model predictions for reaction of methylglyoxal (1 mM) with BSA (100 μM) at physiological pH and temperature. Data (symbols) were obtained from Lo et al. (1994) and are compared with Model #1 predictions (lines) for reaction of MG in this system. For modeling purposes, BSA is treated as a pool of free arginine, lysine and cysteine at concentrations of 2300 μM, 6100 μM and 300 μM, respectively. (a) Degraded MG (1) and free MG (2); (b) irreversibly bound MG (3) and reversibly bound MG (4).

covalently bonded Amadori products. These then undergo further irreversible rearrangements to form AGEs with a broad range of structures.

The first model developed and tested (Model 1; Schematic in Figure 2a) considered MG–protein interactions *in vitro*. The model was tested with data from the study of Lo et al. (1994). This study measures, as a function of time, the relative levels of irreversibly bound, reversibly bound, free and degraded MG present in an *in vitro* system – consisting of MG (100 μM) and BSA (1 mM) at physiological pH and temperature. In this instance, irreversibly bound is a functional definition that represents the MG that has gone through a second reaction step with Arginine and Lysine (MG-Arg_2 and MG-Lys_2 in Figure 2a). Reversibly bound MG represents the MG associated with cysteine and involved in the first reaction step with

Arginine and Lysine (MG-Cys, MG-Arg_1 and MG-Lys_1 in Figure 2a).

Figure 3a shows a comparison of the experimental and predicted levels for free and degraded MG. Figure 3b shows a comparison of the experimental data and the model predictions for irreversibly and reversibly bound MG. Free MG represents MG that remains free and in solution, whether in hydrated or non-hydrated form. Degraded MG represents MG that either spontaneously degraded or dimerized during the course of the original study. Both free and degraded MG were given as model outputs and could be directly compared with experimental results.

Equilibrium constant data for MG interactions with the *N*α-acetylamino acid forms of arginine, lysine and cysteine were obtained from the literature (Lo et al. 1994). The assumption made in using these data was that it would provide a reasonable approximation of interactions between MG and the various amino acid residues. This assumption is less than optimal when considering specific amino acid residues. For example, the equilibrium constant for the MG:*N*α-acetylcysteine interaction ($K_{equil} = 5.6\times10^6\ M^{-1}$; Lo et al. 1994) differs significantly from that of MG:reduced glutathione ($K_{equil} = 2.8\times10^5\ M^{-1}$; Creighton et al. 1988), a tripeptide containing cysteine. However, if the average equilibrium between MG and the pool of available amino acid residues is considered, this assumption appears reasonable as shown in Figure 3.

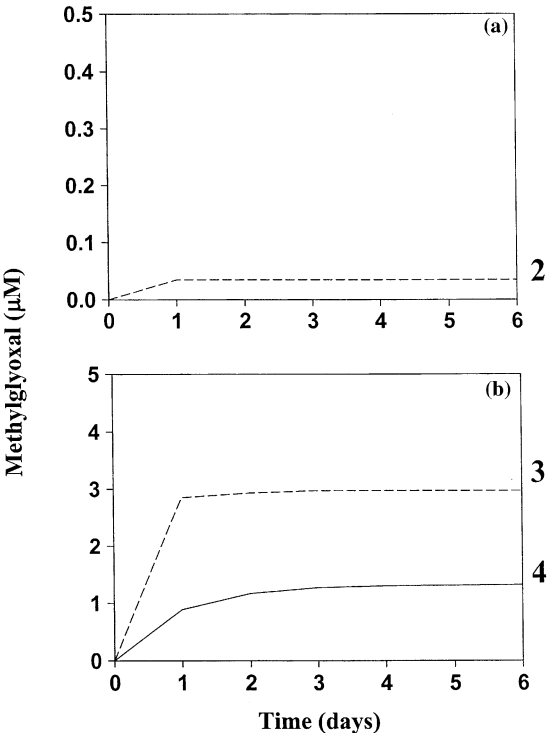

Figure 4. Model predictions for MG modification of intracellular proteins. The model predicts the level of MG associated with cellular arginine, lysine and cysteine residues after a step increase in MG anabolism at $t = 0$. Model parameters were fixed as follows: k_m of glyoxalase I = 200 μM; specific activity of glyoxalase I = 31,000 μmol product/min ml-cell-volume; carbon flux to MG, 5000 μM/day; average protein life, 1 day; [cysteine residue] = 39.74 mM, [arginine residue] = 70.5 mM, [lysine residue] = 105 mM. Assumption is that no chemically degraded methylglyoxal is generated due to low physiological concentrations. (a) Free MG (2); (b) irreversibly bound MG (4) and reversibly bound MG (3).

Table 1. Effect of incubation with *o*-PD at different concentrations.

o-Phenylenediamine concentration (μM)	Reversibly bound methylglyoxal (μM)[a]
0	0
50	17 ± 6
100	32 ± 10
200	60 ± 18
500	148 ± 22
1000	194 ± 44
2000	245 ± 88
5000	306 ± 62

[a]Samples were derivatized at 20 °C in PCA (0.45 M) for 24 h with *o*-PD and then analyzed for 2-MQ content by HPLC. Each datapoint represents mean $\pm 2\sigma$; $n = 6$. See (Chaplen et al., 1998).

Modeling the fate of intracellular MG

Model 1 was extended to include aspects of MG metabolism in cultured cells (Model 2; Schematic in Figure 2b). Intracellular free MG exists as a complex function of cell metabolism and interactions with cellular structures, in particular, proteins (Chaplen et al., 1998). MG:protein interactions form the central element of Model 2 (Figure 2b), where they are treated similarly to Model 1, but with the arginine, lysine and cysteine residue concentrations adjusted to reflect the protein content and composition of mammalian cells. Model 2B only accounts for spontaneously formed MG adducts. Additional terms representing MG anabolism and catabolism, and protein turnover were also added. The resulting model predicts the

effect of step changes in MG anabolism on bound and free intracellular MG levels. MG anabolism was assumed to be zero order and was set at 5000 μmol ml-packed-cell^{-1} day^{-1} based on experimental measurements of D-lactate flux in CHO cells. MG catabolism was assumed to be via the glyoxalase pathway alone since order-of-magnitude estimates have indicated that 10- to 40-fold more MG is detoxified by the glyoxalase system than by aldose reductase in most human tissues (Thornalley 1996). Kinetic data for modeling the glyoxalase I reaction was derived from measurements of specific activity in CHO cells (Chaplen et al. 1996a) and by averaging reported k_m data from various mammalian cell types (Thornalley 1990). Protein turnover was considered first order in protein concentration and was set to give an average protein life of 1 day ($k_t = 1.16 \times 10^{-5}$ s^{-1}).

Figure 4 shows the level of free, reversibly and irreversibly bound MG predicted by the model using the definitions above. The steady-state concentration of free MG was 0.035 μmol L-packed-cell^{-1}; the steady state concentration of reversibly bound MG was 3 μmol L-packed-cell^{-1}; the steady state concentration of irreversibly bound MG was 1.3 μmol L-packed-cell^{-1}. These levels of reversibly bound MG were 1–2 orders of magnitude lower than found in CHO cells in culture (Table 1; Chaplen et al. 1998).

In normal tissues, long-lived proteins, such as eye lens crystallin, accumulate AGEs with age (Ahmed et al. 1997). Even short-lived proteins, such as hemoglobin, can accumulate AGEs, although at lower levels (Makita et al. 1992). The steady state concentration of irreversibly bound MG increased with decreased protein turnover but did not exceed 10 μmol L-packed-cell^{-1} even for an average protein life of 100 days.

MG metabolism dynamics in batch culture

The predicted flux to D-lactate for normal tissues is on the order of 500 μmol ml-packed-cell^{-1} day^{-1}

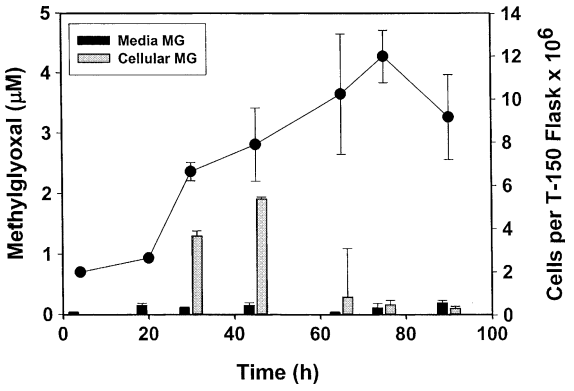

Figure 5. Change in medium and cellular MG levels for CHO cells in batch culture. CHO cells were cultured in T-150 tissue culture flasks. Cells were seeded at 2.0×10^6 cells per flask and cell growth measured through cell counts. Media measurements show consistent levels of free MG present in the system. Cell measurements showed an increase in reversibly bound MG during exponential growth phase and a significant decrease during lag phase.

Table 2. MG metabolism measurements in batch culture[a].

Time (h)	Medium free MG[b] (μM)	Cellular "free" MG[c] (μM)	D-Lactic acid [d] (mM ml-cells^{-1})	D-Lactic acid flux[e] (mM ml-cells^{-1} day^{-1})
0	–	–	0	–
4	0.03 ± 0.01	–	2.64 ± 1.14	16
20	0.15 ± 0.03	–	7.78 ± 0.67	7.7
30	0.11 ± 0.01	1.3 ± 0.08	9.75 ± 0.34	4.7
45	0.15 ± 0.04	1.91 ± 0.03	12.48 ± 1.48	4.4
65	0.03 ± 0.01	0.29 ± 0.8	14.59 ± 0.66	2.5
75	0.11 ± 0.07	0.16 ± 0.07	13.4 ± 2.12	0[f]
90	0.19 ± 0.03	0.1 ± 0.03	13.6 ± 0.80	0.3

[a]All values apart from last column mean $\pm\sigma$; $n = 4$.
[b]Media samples were derivatized at 20 °C in PCA (0.45 M) for 4 h with *o*-PD and then analyzed for 2-MQ content by HPLC.
[c]Cell samples were incubated in PCA for 10 min and the resulting precipitate was removed by centrifugation (25,000 × *g*; 10 min). Samples were derivatized at 20 °C for 4 h with *o*-PD and then analyzed for 2-MQ content by HPLC as described.
[d]D-Lactic acid was fluorometrically determined as described.
[e]D-Lactic acid production was calculated as (Value at t_2 – Value at t_1)/($t_2 - t_1$) from previous column.
[f]Calculated value was less than zero.

(Richard 1991). The measured value for red blood cells is 125 μmol ml-packed-cell^{-1} day^{-1} (Thornalley 1988). The predicted steady state values for free MG ($\sim$0.003 μmol L-packed-cell$^{-1)}$ for this study at 500 μmol ml-packed-cell^{-1} day^{-1} D-lactic acid produced were an order of magnitude below that measured for CHO cells in culture. In addition, levels of bound MG were 2–3 orders of magnitude below those recovered using an assay for reversibly bound MG (Chaplen et al. 1998; Table 1). Table 2 reports measurements of D-lactic acid flux in CHO cells grown in culture ranged from 15.8 mmol ml-packed-cell^{-1} day^{-1} in lag phase to 0 mmol ml-packed-cell^{-1} day^{-1} in stationary phase and were greatest in lag and early exponential phase. Table 2 also reports measurements for medium MG – representative of free MG levels in cell increased during exponential and late stationary phase and ranged from 0.03 ± 0.01 to 0.19 ± 0.04 μmol L-packed-cell^{-1} (mean $\pm$ std. dev; $n = 4$). Medium measurements of free MG are better predictors of cellular MG levels because MG is freely membrane permeable and the assay for free intracellular MG also captures some reversibly bound MG. The predicted levels of free MG were consistent with these values (0.03–0.1 μmol L-packed-cell^{-1}). However, the predicted values for bound MG (maximum 10 μmol L-packed-cell^{-1} at an average protein life of 100 days) were still 1–2 orders of magnitude the values observed from the assay for reversibly bound MG. Figure 5 shows measurements for free cellular MG in relation to the culture phase – which capture both free and some reversibly bound MG ranged from 0.1 ± 0.03 to 1.9 ± 0.03 μmol L-packed-cell^{-1} (mean $\pm$ std. dev; $n = 4$) with a maximum in exponential phase growth. These values are higher than those reported for the medium because the intracellular assay for free MG also captures some reversibly bound MG (Chaplen et al. 1996b).

Discussion

The culturing of mammalian cells is an important technology for the commercial production of high value proteins, such as interleukins, interferon, tissue plasminogen activator and monoclonal antibodies. Cell lines must provide a consistent product and high specific productivities for long periods of time. Premature cell death in industrial cell cultures represents a significant loss of valuable resources and has important consequences for overall process productivity. Much effort is focused on enhancing cell survival in industrial cell culture with various genetic, chemical or nutritional approaches. High levels of reversibly bound MG can be recovered from CHO cells grown in culture (AGE and AGE precursors). Furthermore, CHO and other cell-lines used in industrial cell culture contain many of the elements (signal molecules, kinases, receptors) reported to participate in the MG-dependent cell death pathways, and the negative effects of endogenous MG accumulation on CHO cell viability is demonstrated. Previous studies to model MG metabolism focused on the kinetics of the glyoxalase system (cf. Creighton et al. 1988; Martins et al. 2001). In this work, a kinetic model that qualitatively describes the distribution of spontaneously reacting MG with proteins was developed and validated in order to better understand MG metabolism in cultured CHO cells.

MG modification of cellular proteins

Model 1 allowed validation of the general approach for modeling spontaneous modification of protein amino acids. Model 2 models the spontaneous formation of protein:MG AGEs in cellular systems. The spontaneous formation of AGEs may have significant implications for cell function in culture due to the MG-mediated cell death pathways. AGE-modified proteins are antigenic and provoke cellular injury responses upon endocytosis by cell-surface receptors. Several MG-derived AGEs have been identified, including N^{ϵ}-(carboxyethyl)-lysine (CEL), MG-lysine dimer (MOLD), argpyrimidine, and 5-methylimidazolone (Bourajjaj et al. 2003). Cysteine modification results in the formation of a highly unstable hemithioacetal, which then may be transformed to irreversible AGE-like adducts, a reaction mediated by phosphorylated GLO1 (Van Herreweghe et al. 2002). MG modification of N-terminal amino acids results in their rapid deamination ((Takahashi 1968). Modification of nucleic acids occurs principally at guanyl bases (Vaca et al. 1994), and results in gene mutation and abnormal gene expression patterns (Papsoulis et al. 1995). Oxi-

dative stress, mediated through ROS, magnifies the mutagenicity of MG many-fold. Little is yet understood about interactions between intracellular metabolic fluxes and fluxes to individual AGES.

MG and cell death

MG metabolism is 1–2 orders of magnitude more active in CHO cells during certain phases of batch culture than in normal tissues. A high rate of detoxification during lag phase is evident from Table 2. Low rates of detoxification occur during stationary phase. These results are consistent with the possible role of MG in modulating cell growth and function in batch culture. The level of reversibly bound MG predicted by Model 2 is 1–2 orders of magnitude less than that measured using an assay designed to capture reversibly bound MG (Table 1). This suggests that much of the MG-derived adduct formation that occurs in the cell is tightly regulated and involved in the regulation of cellular activities.

The link between endogenous MG and cell death is firmly established in several cell lines (Jurkat leukemia, HL60, human myeloma U266, murine fibrosarcoma L929). The cellular machinery associated with MG-mediated cell death has only been partially elucidated, however. MG-mediated cell death in L929 cells is initiated through TNF-α binding to cell surface receptors. The process in L929 cells is caspase independent and characterized by mitochondrial accumulation of ROS (Van Herreweghe et al. 2002). Activation of protein kinase A (PKA) by TNF-α leads to phosphorylation of GLO1. Increased MG anabolism is also evident in L929 cells exposed to TNF-α resulting in increased levels of endogenous MG. Phosphorylated GLO1 then modifies specific and as yet unidentified protein sites in the cell to form novel AGE's. The structure of these modifications has not been elucidated. Basal levels of phosphorylated GLO1 are always present in the cell, but increased levels are generated in response to cellular exposure to TNF-α. Addition of anti-oxidants significantly decreases the level of GLO1-mediated cell death indicating that mitochondrial ROS accumulation plays a critical role. Considerable 'cross-talk' between the various signaling pathways associated with MG and cell death in L929 cells is also evident. Caspase inhibitors block Fas-mediated apoptotic death in L929 cells but ultimately result in necrotic cell death mediated through accumulation of ROS. Inhibition of caspase activities sensitizes the cells to TNF-α-mediated necrotic cell death. Caspases may have a role as negative regulators of TNF-α-induced radical formation in the mitochondria of L929 cells. Oxidative damage to intracellular proteins increases their susceptibility to proteolysis. A low level of caspase activity may be beneficial to the cell imparting protection to mitochondria damaged by increased levels of ROS.

There are also reports of the mechanisms of MG-mediated cell death in other cell lines that give strong indications of involvement in cell death processes in general. MG modification prevents Hsp27 oligomerization followed by cytochrome c-mediated caspase activation and apoptotic cell death in human leukemia U937 cells (Sakamoto et al. 2000). MG-mediated cell death in the human myeloma cell line U266 contrasts with that in L929 cells in that it is caspase dependent, although it does not involve the mitogen activating protein (MAP) kinase pathway. Rather, activation of protein kinase C (PKC) by MG leads to ROS accumulation and apoptotic cell death. PKC activation is not dependent on the presence of ROS. MG-mediated cell death in the human Jurkat leukemia cell line is also caspase dependent (8). Activation of c-Jun N-terminal kinase (JNK) by MG leads to caspase-3 activation and subsequent apoptosis. Inhibition of JNK by curcumin or expression of a dominant negative mutant of JNK protected the cells from MG-induced apoptosis. Finally, increased levels of endogenously produced MG have been associated with apoptosis in HL60 cells exposed to the GLO1 inhibitor diester *S-p*-bromobenzylglutathione diester (BBGD; Thornalley et al. 1996). This contrasts with the increase in necrosis noted in L929 cells after exposure BBGD.

Conclusions

Mammalian cell culture is an important technology for the production of therapeutic proteins. Cells grown in culture produce a number of toxic by-products that are known to reduce cell productivity. Two major inhibitory waste-products are L-lactate and ammonium ion. MG is a less

well-known inhibitory compound, found in mammalian systems as a consequence of glycolysis and other anabolic processes. MG is of potential biotechnological interest because it is a potent protein and nucleic acid modifying agent and a cause of general oxidative stress, producing ROS. The majority of intracellular MG (>99%) is associated with macromolecules, particularly proteins and nucleic acids. Endogenously produced MG is a mediator in certain cell death pathways. Kinetic modeling results from this study suggest that most bound MG is non-spontaneously associated with proteins.

Acknowledgements

We thank the Whitaker Foundation for research support. We thank John Bolte and Douglas Cameron for many useful discussions.

References

Ahmed M.U., Brinkmann Frye E., Degenhardt T.P., Thorpe S.R. and Baynes J.W. 1997. N-ε-(carboxyethyl)lysine, a product of the chemical modification of proteins by methylglyoxal, increases with age in human lens proteins. Biochem. J. 324: 565–70.

Alberts G., Bray D., Lewis J., Raff M., Roberts K. and Watson J.D. 1994. Molecular Biology of the Cell, 3rd ed. Garland Publishing Inc., New York.

Anderson D.C. and Goochee C.F. 1995. The effect of ammonia on *O*-linked glycosylation of granulocyte colony-stimulating factor produced by Chinese hamster ovary cells. Biotechnol. Bioeng. 47: 96–105.

Bibila T.A. and Robinson D.K. 1995. In pursuit of the optimal fed-batch process for monoclonal antibody production. Biotechnol. Prog. 11: 1–13.

Bourajjaj M., Stehouwer C.D.A., van Hinsbergh V.W.M. and Schalkwijk C.G. 2003. Role of methylglyoxal adducts in the development of vascular complications in diabetes mellitus. Biochem. Soc. Trans. 31(6): 1400–1402.

Chaplen F.W.R., Cameron D.C. and Fahl W.E. 1996a. Effect of endogenous methylglyoxal on Chinese hamster ovary cells grown in culture. Cytotechnology 22: 33–42.

Chaplen F.W.R., Fahl W.E. and Cameron D.C. 1996b. Method for determination of free extracellular and intracellular methylglyoxal in animal cells grown in culture. Anal. Biochem. 238: 171–178.

Chaplen F.W.R., Fahl W.E. and Cameron D.C. 1998. Evidence of high levels of methylglyoxal in Chinese hamster ovary cells grown in culture. Proc. Natl. Acad. Sci. USA 95: 5533–5538.

Creighton D.J., Migliorine M., Pourmotabbed T. and Guha M.K. 1988. Optimization of the efficiency of the glyoxalase pathway. Biochemistry 27(19): 7376–84.

Du J., Suzuki H., Nagase F., Akhand A.A., Yokoyama T., Miyata T., Kurokawa K. and Nakashima I. 2000. Methylglyoxal induces apoptosis in Jurkat leukemia cells by activating c-Jun N-terminal kinase. J. Cell. Biochem. 77(2): 333–44.

Godbout J.P., Pesavento J., Hartman M.E., Manson S.R. and Freund G.G. 2001. Methyglyoxal enhances cisplatin-induced cytotoxicity by activating PKC-δ. J. Biol. Chem. 277(4): 2554–2561.

Jocelyn P.C. 1977. Biochemistry of the SH Group. Academic Press, New York.

Lo T.W.C., Westwood M.E., McLellan A.C., Selwood T. and Thornalley P.J. 1994. Binding and modification of proteins by methylglyoxal under physiological conditions. J. Biol. Chem. 269: 32299–32305.

Makita Z., Vlassara H. and Cerami A. and Bucala R. 1992. Immunochemical detection of advanced glycosylation end products *in vivo*. J. Biol. Chem. 267(8): 5133–5138.

Martins A.M., Mendes P., Cordeiro C. and Freire A.P. 2001. In situ kinetic analysis of glyoxalase I and glyoxalase II in *Saccharomyces cerevisiae*. Eur. J. Biochem. 268(14): 3930–3936.

McLellan A.C., Phillips S.A. and Thornalley P.J. 1992. Fluorimetric assay of D-lactate. Anal. Biochem. 206(1): 12–6.

Miller W.M. and Blanch H.W. 1991. Regulation of animal cell metabolism in bioreactors. In: Ho C.S and Wang D.I.C. (eds), Animal Cell Bioreactors, Ch. 6. Butterworth-Heinemann, Boston, pp. 119–157.

Papsoulis A., Al-Abed Y. and Bucala R. 1995. Identification of N2-(1-carboxyethyl)guanine (CEG) as a guanine advanced glycosylation end-product. Biochemistry 34: 648–655.

Richard J.P. 1991. Kinetic parameters for the elimination reaction catalyzed by triosephosphate isomerase and an estimation of the reaction′s physiological significance. Biochemistry 30: 4581–4585.

Sakamoto H., Mashima T., Kizaki A., Dan S., Hashimote Y., Naito M. and Tsuruo T. 2000. Glyoxalase I is involved in the resistance of human leukemia cells to antitumor agent-induced apoptosis. Blood 95(10): 3214–3218.

Shamsi F.A., Partal A., Sady C., Glomb M.A. and Nagaraj R.H. 1998. Immunological evidence for methylglyoxal-derived modifications *in vivo*. Determination of antigenic epitopes. J. Biol. Chem. 273(12): 6928–6936.

Shinohara M., Thornalley P.J. and Giadino I. et al. 1998. Overexpression of glyoxalase I in bovine endothelial cells inhibits intracellular advanced glycation end-product formation and prevents hyperglycemia-induced increases in macromolecular endocytosis. J. Clin. Invest. 101(5): 1142–1147.

Takahashi K. 1968. The reaction of phenylglyoxal with arginine residues in proteins. J. Biochem. (Tokyo) 23: 6171–6179.

Thornalley P.J. 1988. Modification of the glyoxalase system in human red blood cells by glucose *in vitro*. Biochem. J. 254: 751–755.

Thornalley P.J. 1990. The glyoxalase system: new developments towards functional characterization of a metabolic pathway fundamental to biological life. Biochem. J. 269: 1–11.

Thornalley P.J. 1996. Pharmacology of methylglyoxal: formation, modification of proteins and nucleic acids, and enzymatic detoxification – a role in pathogenesis and antiproliferative chemotherapy. Gen. Pharmacol. 27(4): 565–573.

Thornalley P.J., Edwards L.G., Kang Y., Wyatt C., Davies N., Ladan M.J. and Double J. 1996. Antitumor activity of *S*-p-bromobenzylglutathione cyclopentyl diester *in vitro* and *in vivo*. Inhibition of glyoxalase I and the induction of apoptosis. Biochem. Pharmacol. 51(10): 1365–1372.

Vaca C.E., Fang J-L., Conradi M. and Hou S-M. 1994. Development of a ^{32}P-postlabelling method for the analysis of 2′-deoxyguanosine-3′-monophosphate and DNA adducts of methylglyoxal. Carcinogenesis 15: 1887–1894.

Vander Jagt D.L., Hassebrook R.K., Hunsaker L.A., Brown W.M. and Royer R.E. 2001. Metabolism of the 2-oxoaldehyde methylglyoxal by aldose reductase and by glyoxalase-I: roles for glutathione in both enzymes and implications for diabetic complications. Chem. Biol. Interact. 130–132(13): 549–562.

Vander Jagt D.L., Han L.P. and Lehman C.H. 1972. Kinetic evaluation of substrate specificity in the glyoxalase I disproportionation of α-ketoaldehydes. Biochemistry 11(20): 3735–3740.

Van Herreweghe F., Mao J., Chaplen F.W.R., Grooten J., Gevaert K., Vandekerckhove J. and Vancompernolle K. 2002. Tumor Necrosis Factor-induced modulation of glyoxalase I activities through phosphorylation by PKA results in cell death and is accompanied by the formation of specific methylglyoxal-derived AGEs. Proc. Natl. Acad. Sci. USA 99(2): 949–954.

Uchida K., Khor O.T., Oya O., Osawa T., Yasuda Y. and Miyata T. 1997. Protein modification by Maillard reaction intermediate methylglyoxal. Immunochemical detection of fluorescent 5-methylimidazolone derivatives *in vivo*. FEBS Lett. 410(2–3): 313–318.

Westwood M.E., McLellan A.C. and Thornalley P.J. 1994. Receptor-mediated endocytic uptake of methylglyoxal-modified serum albumin. J. Biol. Chem. 269: 32293–32298.

Westwood M.E. and Thornalley P.J. 1996. Induction of synthesis and secretion of interleukin 1β in the human monocyteic THP-1 cells by human serum albumins modified by methylglyoxal and advanced glycation endproducts. Immunol. Lett. 50: 17–21.

Xie L. and Wang D.I. 1994. Applications of an improved stoichiometric model in medium design and fed-batch cultivation of animal cells in a bioreactor. Cytotechnology 15(1–3): 17–29.